

Supporting Information for

Ultrahigh-Resolution ^7Li MAS NMR Spectroscopy by Isotopic Dilution

Vladimir K. Michaelis,^{a,†,*} Kirill Levin,^a Yaroslav Germanov,^a Gérald Lelong^b and Scott Kroeker^{a,*}

¹*Department of Chemistry, University of Manitoba, Winnipeg, Manitoba, Canada, R3T 2N2*

²*Institut de Minéralogie de Physique des Matériaux et de Cosmochimie (IMPMC), Sorbonne Universités – UPMC, Jussieu, 75005, Paris, France*

*Corresponding Authors: Vladimir Michaelis, vladimir.michaelis@ualberta.ca; Scott Kroeker, Scott.Kroeker@umanitoba.ca

TABLE OF CONTENTS

Materials and Methods	3
Figure S1: ${}^7\text{Li}$ MAS NMR spectra of lithium orthoborate, Li_3BO_3 : (a) depleted sample ($\nu_r=60$ kHz, $B_o = 11.7$ T, 5% ${}^7\text{Li}$), (b) depleted sample ($\nu_r=16$ kHz, $B_o = 14.1$ T, 5% ${}^7\text{Li}$), and (c) natural abundance sample ($\nu_r=60$ kHz, $B_o = 11.7$ T, 92.5% ${}^7\text{Li}$).	4
Figure S2: ${}^{67}\text{Li}$ MAS NMR spectra of $\text{Li}_6\text{B}_4\text{O}_9$ at 11.7 T, a spinning frequency of 60 kHz (3 mgs, 1.3 mm o.d. rotor) and between 4 and 32 co-added transients. (a) ${}^6\text{Li}$ MAS NMR of natural abundance sample (acq. time, ~ 3 hrs), (b) ${}^6\text{Li}$ MAS NMR of depleted sample (acq. time ~ 15 hrs), (c) ${}^7\text{Li}$ MAS NMR of natural abundance sample (acq. time ~ 3 min) and (d) ${}^7\text{Li}$ MAS NMR of depleted sample (acq. time ~ 24 min).	4
Figure S3: ${}^7\text{Li}$ MAS NMR EXSY spectrum of $\text{Li}_6\text{B}_4\text{O}_9$ ($\nu_r=60$ kHz, 11.7 T) acquired with a 40-second mixing time.	5
Figure S4: ${}^7\text{Li}$ isotropic chemical shift as a function of geometry index, τ , defined by the difference between the largest bond angle, β , and second-largest bond angle, α , as shown; ideal square-pyramidal geometry corresponds to $\tau = 0$ and ideal trigonal-bipyramidal geometry corresponds to $\tau = 1$. ¹	5
Figure S5. ${}^7\text{Li}$ MAS NMR ($B_0 = 14.1$ T, $\nu_r=16$ kHz) of lithium borate glasses with compositions specified by $R=\text{Li}_2\text{O}/\text{B}_2\text{O}_3$: (a) $R = 0.1$, ${}^7\text{Li}$ depleted, (b) $R = 0.1$, natural abundance, (c) $R = 1.0$, ${}^7\text{Li}$ depleted, (d) $R = 1.0$, natural abundance.	6
Table S1: ${}^7\text{Li}$ MAS NMR experimental (depleted, 5% ${}^7\text{Li}$) and GIPAW-calculated parameters for crystalline lithium borates.	7
Table S2: ${}^7\text{Li}$ MAS NMR parameters for crystalline lithium borates prepared in natural abundance (92.5% ${}^7\text{Li}$) and isotopically diluted (5% ${}^7\text{Li}$)	7
Table S3: ${}^7\text{Li}$ MAS NMR parameters for a series of natural abundance (92.5% ${}^7\text{Li}$) and depleted (5% ${}^7\text{Li}$) lithium borate glasses.	8
References	8

MATERIALS & METHODS

Materials: Natural abundance samples (92.5% ^7Li , 7.5% ^6Li) were synthesized using >99 % Li_2CO_3 (Sigma-Aldrich, St. Louis, USA). ^7Li -depleted samples were prepared using isotopically enriched $^6\text{Li}_2\text{CO}_3$ (95% ^6Li , 5% ^7Li , Sigma-Aldrich, St. Louis, USA). For all samples, the initial powdered mixture was heated to 700°C for a few hours and weighed to confirm completion of decarbonation. All borates were synthesized using stoichiometric amounts of B_2O_3 - made from the dehydration of H_3BO_3 - and lithium carbonate (Li_2CO_3). Natural abundance and depleted lithium metaborate (LiBO_2) and lithium orthoborate (Li_3BO_3) samples were made by high-temperature synthesis. The first heat treatment involved heating to 900 °C and cooling to room temperature. After regrinding, the sample was heated to 850 °C for 64 hours, followed by a slow annealing process (cooling at ~ 30 °C/hr) to 200 °C to improve crystallinity. Natural abundance and ^7Li -depleted $\text{Li}_6\text{B}_4\text{O}_9$ were synthesized as previously described by Rouse et al.² The identity and purity of all crystalline products were confirmed using powder X-ray diffraction.

Lithium borate glasses were prepared using stoichiometric amounts of B_2O_3 (from dehydrated boric acid) and lithium carbonate (Li_2CO_3), and mixed using an agate mortar and pestle under dry nitrogen (glove box). Each sample was made in duplicate using either 92.5% $^7\text{Li}_2\text{CO}_3$ (natural abundance) or 5% $^7\text{Li}_2\text{CO}_3$ (isotopically depleted). The samples were decarbonated between 500 and 700 °C in a Pt/Au(5%) 15 mL crucible for 1 hour (confirmed by mass loss measurements). The decarbonated mixtures were then placed into a box furnace set between 900 and 1000 °C for 20 minutes to form a homogeneous melt, followed by a rapid quenching using deionized H_2O . A reduction in batch size for the R=1.0 glass was needed (75 mg vs. 200-400 mg) to prevent the formation of crystallization during water quenching.

Solid-State Nuclear Magnetic Resonance (NMR) Spectroscopy: Lithium-7 NMR spectra were acquired on a Varian ^{UNITY}Inova or a Bruker Avance III HD NMR spectrometer equipped with either a 14.1 T (600 MHz, ^1H) Oxford or 11.7 T (500 MHz, ^1H) Bruker superconducting magnet, respectively. All NMR spectra were collected under magic-angle spinning (MAS) using either a 3.2 mm double-resonance (H/F-X) Varian-Chemagnetics or a 1.3 mm double-resonance (H-X) Bruker probe. All samples were powdered using an agate mortar and pestle, and packed into 3.2 or 1.3 mm o.d. ZrO_2 rotors. Spectra were acquired with a single-pulse (Bloch³) sequence using a 0.5 μs pulse ($\sim 13^\circ$ tip angle), 16 to 512 co-added transients, recycle delays between 10 and 500 seconds and spinning frequencies ranging between 6 and 65 kHz. ^7Li two-dimensional exchange spectroscopy (2D EXSY⁴) spectra were acquired at a spinning frequency of 60 kHz with $\pi/2$ pulses of 2.9 μs , recycle delays of 125 s, 8 co-added transients and 64 t_1 increments; mixing times ranged from 0.1 to 40 seconds, depending on the sample. All spectra were externally referenced to 1 M LiCl at 0 ppm.⁵ Relaxation measurements for the lithium environments were carried out using a saturation-recovery pulse sequence $((90^0)_n-90^0)$ $(90-t_1)_n-$ τ -90-acq, with the pulse train, $n = 24$ to ensure complete saturation.^{6,7} The pulse trains were solid 90° pulses of 3.75 μs ($\sqrt{B_1}/2\pi = 67$ kHz) with delays between pulses of 20 ms and varying τ -values between 1 to 20,000 seconds. Sample temperatures were calibrated using $\text{Pb}(\text{NO}_3)_2$ based on the ^{207}Pb chemical shift data,^{8,9} to account for frictional heating. ^6Li MAS NMR spectra (14.1 T) of the depleted samples (95% ^6Li) were collected to compare the sensitivity and resolution of natural-abundance and ^7Li -depleted samples. Spectra were acquired with a Bloch pulse and a 1 μs pulse ($\sim 18^\circ$ tip angle, $\sqrt{B_1}/2\pi=50$ kHz), using between 4 and 64 co-added transients, recycle delays between 500 and 15,000 seconds and a spinning frequency of 16 kHz.

Quantum Chemical Calculations: Magnetic shielding calculations were performed using Gauge Including Projector Augmented Waves (GIPAW), a density-functional theory (DFT) method as implemented in the CASTEP software (ver. 4.4) at the Ultrahigh Field NMR Facility for Solids (Ottawa, Canada).¹⁰ The Perdew-Burke-Ernzerhof (PBE) functionals were used in the generalized gradient approximation (GGA) for the exchange-correlation energy^{11,12} with ultrasoft pseudopotentials¹³ generated on the fly. Calculations were performed using geometries determined from their respective x-ray diffraction structures.^{2,14-16} All NMR calculations were performed with a medium accuracy basis set and a maximum plane-wave energy of 500 eV. The Monkhorst-Pack grid had a maximum density between $2 \times 2 \times 2$ and $4 \times 3 \times 2$ k points (2 to 4 k points) depending on the structure. Calculated magnetic shieldings were converted to isotropic chemical shifts using the following equation, $\delta_{\text{iso}} = -(\sigma_{\text{iso}} - \sigma_{\text{ref}})$, where $\sigma_{\text{ref}} = 89.939$ ppm, obtained from linear regression of the calculated and experimentally determined isotropic chemical shifts (Figure S7).

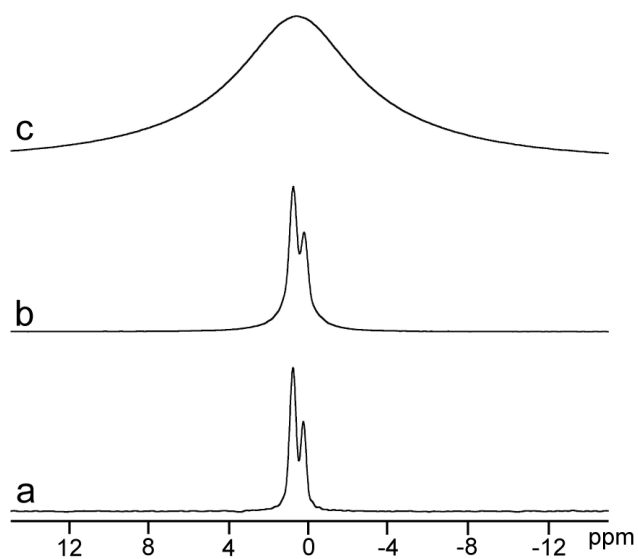


Figure S2. ^7Li MAS NMR spectra of lithium orthoborate, Li_3BO_3 : (a) depleted sample ($\nu_r=60$ kHz, $B_o = 11.7$ T, 5% ^7Li), (b) depleted sample ($\nu_r=16$ kHz, $B_o = 14.1$ T, 5% ^7Li), and (c) natural abundance sample ($\nu_r=60$ kHz, $B_o = 11.7$ T, 92.5% ^7Li).

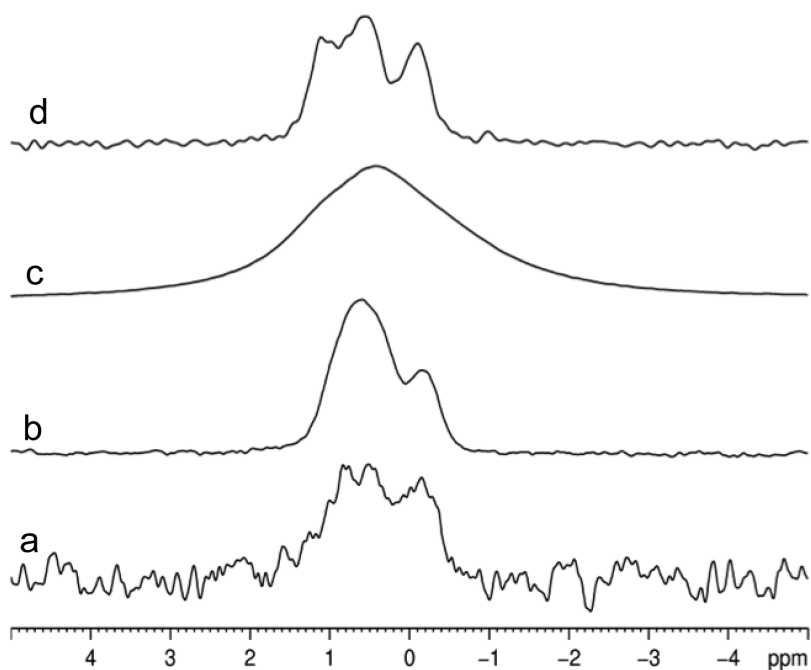


Figure S2. $^{6/7}\text{Li}$ MAS NMR spectra of $\text{Li}_6\text{B}_4\text{O}_9$ at 11.7 T, a spinning frequency of 60 kHz (3 mg, 1.3 mm o.d. rotor) and between 4 and 32 co-added transients. (a) ^6Li MAS NMR of natural abundance sample (acq. time, ~ 3 hrs), (b) ^6Li MAS NMR of depleted sample (acq. time ~ 15 hrs), (c) ^7Li MAS NMR of natural abundance sample (acq. time ~ 3 min) and (d) ^7Li MAS NMR of depleted sample (acq. time ~ 24 min).

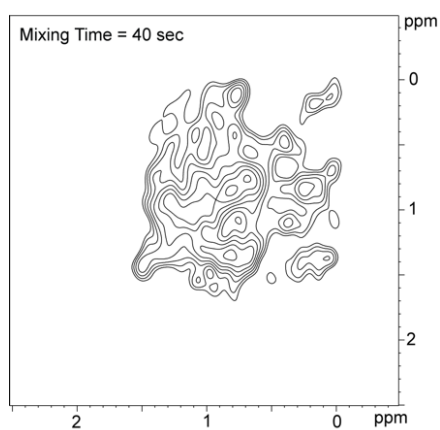


Figure S3. ^7Li MAS NMR EXSY spectrum of $\text{Li}_6\text{B}_4\text{O}_9$ ($\nu_r=60$ kHz, 11.7 T) acquired with a 40-second mixing time.

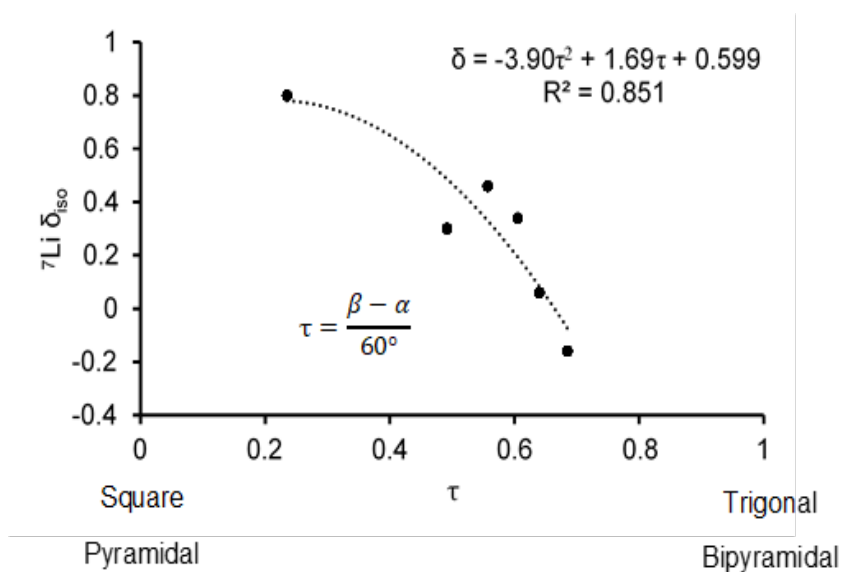


Figure S4. ^7Li isotropic chemical shift as a function of geometry index, τ , defined by the difference between the largest bond angle, β , and second-largest bond angle, α , as shown; ideal square-pyramidal geometry corresponds to $\tau = 0$ and ideal trigonal-bipyramidal geometry corresponds to $\tau = 1$.¹

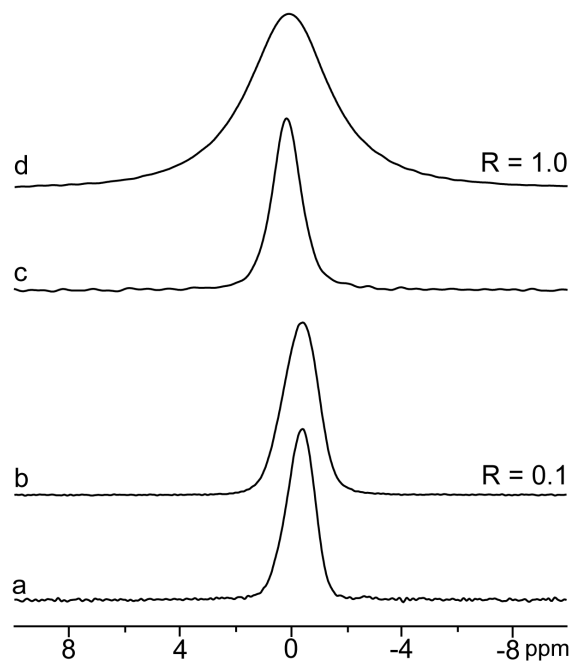


Figure S5. ${}^7\text{Li}$ MAS NMR ($B_0 = 14.1$ T, $\nu_r = 16$ kHz) of lithium borate glasses with compositions specified by $R = \text{Li}_2\text{O}/\text{B}_2\text{O}_3$: (a) $R = 0.1$, ${}^7\text{Li}$ depleted, (b) $R = 0.1$, natural abundance, (c) $R = 1.0$, ${}^7\text{Li}$ depleted, (d) $R = 1.0$, natural abundance.

Table S2. ^7Li MAS NMR experimental (depleted, 5% ^7Li) and GIPAW-calculated parameters for crystalline lithium borates.

Sample	Site	CN	δ_{iso} (ppm)		$\sigma_{\text{iso}}^{\text{a}}$ (ppm)	T_1 (s) ^c	
			exp. ± 0.01	calc. ^a			
LiBO_2^{b}	1	5	0.30	0.15	89.788	130 ± 7	1060 ± 180
$\text{Li}_3\text{BO}_3^{\text{b}}$	1	5	0.75	0.64	89.304	90 ± 6	310 ± 34
	2	4	0.97	0.95	88.988		
	3	5	0.33	0.32	89.614		
$\text{Li}_6\text{B}_4\text{O}_9^{\text{b}}$	1	5	0.06	-0.01	89.948	136 ± 9	
	2	4	0.94	1.03	88.913		
	3	5	0.46	0.63	89.309		
	4	5	-0.16	-0.07	90.009		
	5	4	0.69	0.79	89.149		
	6	4	1.14	1.20	88.743		

^a GIPAW calculations

^b ^7Li quadrupole coupling constants (C_{QS}) were estimated experimentally by measuring the satellite transition spinning sideband envelope, and also calculated, to be between 100 and 250 kHz.

^c T_1 values (seconds) for LiBO_2 and Li_3BO_3 were best fit using a bi-exponential, while a mono-exponential fit was suitable for $\text{Li}_6\text{B}_4\text{O}_9$. T_1 values were measured for both depleted and natural abundance samples to assess the contribution of dipolar vs quadrupolar relaxation. The values agreed within experimental uncertainty, indicating that the quadrupolar interaction dominates the spin-lattice relaxation in these systems.

Table S2. ^7Li MAS NMR parameters for crystalline lithium borates prepared in natural abundance (92.5% ^7Li) and isotopically diluted (5% ^7Li)

Sample	Natural Abundance		^7Li Depleted	
	δ_{iso} (ppm) ± 0.1	FWHM (Hz) ± 20	δ_{iso} (ppm) ± 0.01	FWHM (Hz) ± 5
LiBO_2^{a}	0.1	1030	0.49	150
$\text{Li}_3\text{BO}_3^{\text{a}}$	0.6	1300	0.81,0.30	230 ^d
$\text{Li}_6\text{B}_4\text{O}_9^{\text{b}}$	0.4	1200 ^c 460 ^e	-0.16, 0.06, 0.46, 0.69, 0.94, 1.14	270 ^{d,e}

^a $B_0 = 14.1$ T; ^b $B_0 = 11.7$ T; ^c $\nu_r = 16$ kHz; ^d line width of the full resonance (all sites); ^e $\nu_r = 60$ kHz

Table S3. ^7Li MAS NMR parameters for a series of natural abundance (92.5% ^7Li) and depleted (5% ^7Li) lithium borate glasses.

Sample, R^i	Natural Abundance		Depleted	
	δ_{iso} (ppm) ± 0.1	FWHM (Hz) ± 20	δ_{iso} (ppm) ± 0.01	FWHM (Hz) ± 5
0.1	-0.4	350	-0.43	268
0.5	-0.2	570	-0.16	302
0.8	0.1	690	0.10	280
1	0.1	790	0.13	279
2	0.5	1100	0.56	204

ⁱ $R = \text{Li}_2\text{O}/\text{B}_2\text{O}_3$

REFERENCES

- Addison, A. W.; Rao, T. N.; Reedijk, J.; van Rijn, J.; Verschoor, G. C., Synthesis, Structure, and Spectroscopic Properties of Copper(II) Compounds Containing Nitrogen-Sulphur Donor Ligands; the Crystal and Molecular Structure of Aqua[1,7-Bis(N-Methylbenzimidazol-2[Prime or Minute]-Yl)-2,6-Dithiaheptane]Copper(II) Perchlorate. *J. Chem. Soc., Dalt. Trans.* **1984**, (7), 1349-1356.
- Rousse, G.; Baptiste, B.; Lelong, G., Crystal Structures of $\text{Li}_6\text{B}_4\text{O}_9$ and $\text{Li}_3\text{B}_{11}\text{O}_{18}$ and Application of the Dimensional Reduction Formalism to Lithium Borates. *Inorg. Chem.* **2014**, 53 (12), 6034-6041.
- Bloch, F.; Hansen, W. W.; Packard, M., The Nuclear Induction Experiment. *Phys. Rev.* **1946**, 70 (7-8), 474.
- Jeener, J.; Meier, B. H.; Bachmann, P.; Ernst, R. R., Investigation of Exchange Processes by Two-Dimensional NMR Spectroscopy. *J. Chem. Phys.* **1979**, 71 (11), 4546-4553.
- Harris, R. K.; Becker, E. D.; Cabral de Menezes, S. M.; Goodfellow, R.; Granger, P., NMR Nomenclature: Nuclear Spin Properties and Conventions for Chemical Shifts (IUPAC Recommendations 2001). *Solid State Nucl. Magn. Reson.* **2002**, 22, 458.
- Slichter, C. P., *Principles of Magnetic Resonance*. Harper & Row: New York, 1963.
- Bloembergen, N.; Purcell, E. M.; Pound, R. V., Relaxation Effects in Nuclear Magnetic Resonance Absorption. *Phys. Rev.* **1948**, 73 (7), 679.
- Bielecki, A.; Burum, D. P., Temperature Dependence of ^{207}Pb MAS Spectra of Solid Lead Nitrate. An Accurate, Sensitive Thermometer for Variable-Temperature MAS. *J. Magn. Reson.* **1995**, 116 (2), 215-220.
- van Gorkom, L. C. M.; Hook, J. M.; Logan, M. B.; Hanna, J. V.; Wasylishen, R. E., Solid-State Lead-207 NMR of Lead(II) Nitrate: Localized Heating Effects at High Magic Angle Spinning Speeds. *Magn. Reson. Chem.* **1995**, 33 (10), 791-795.
- Segall, M. D.; Lindan, P. J. D.; Probert, M. J.; Pickard, C. J.; Hasnip, P. J.; Clark, S. J.; Payne, M. C., First-Principles Simulation: Ideas, Illustrations and the CASTEP Code. *J. Phys. Condens. Matter* **2002**, 14, 2717.
- Perdew, J. P.; Burke, K.; Ernzerhof, M., General Gradient Approximation Made Simple. *Phys. Rev. Lett.* **1996**, 77 (18), 3865-3868.
- Perdew, J. P.; Burke, K.; Ernzerhof, M., Perdew, Burke, and Ernzerhof Reply. *Phys. Rev. Lett.* **1998**, 80 (4), 891-891.
- Vanderbilt, D., *Phys. Rev. B* **1990**, 41, 7892.
- Zachariasen, W. H., The Crystal Structure of Lithium Metaborate. *Acta Cryst.* **1964**, 17, 749.
- Stewner, V. F., Die Kristallstruktur Von $\alpha\text{-Li}_3\text{BO}_3$. *Acta Cryst.* **1971**, B27, 904.
- Lelong, G.; Radtke, G.; Cormier, L.; Bricha, H.; Rueff, J.-P.; Ablett, J. M.; Cabaret, D.; Gélébart, F.; Shukla, A., Detecting Non-Bridging Oxygens: Non-Resonant Inelastic X-Ray Scattering in Crystalline Lithium Borates. *Inorg. Chem.* **2014**, 53 (20), 10903-10908.

